

## PICARD: SOLAR DIAMETER MEASURE AND g-MODE SEARCH

L. Damé<sup>1</sup>, T. Appourchaux<sup>2</sup>, G. Berthomieu<sup>3</sup>, P. Boumier<sup>4</sup>, D. Cugnet<sup>1</sup>, B. Gelly<sup>5</sup>, J. Provost<sup>4</sup>, T. Toutain<sup>4</sup>

<sup>1</sup>*Service d'Aéronomie du CNRS, BP 3, F-91371 Verrières-le-Buisson Cedex, France*

Tel: +33 1 64474328, Fax: +33 1 69202999, e-mail: luc.dame@aerov.jussieu.fr

<sup>2</sup>*ESTEC, Space Science Department, Postbus 299, NL-2200, AG-Noordwijk, The Netherlands*

<sup>3</sup>*Observatoire de Nice, Département Cassini, BP 4229, F-06304 Nice Cedex 4, France*

<sup>4</sup>*Institut d'Astrophysique Spatiale, Université Paris XI, Bât. 121, F-91405, Orsay Cedex, France*

<sup>5</sup>*Université de Nice (CNRS UMR 6525), Sophia Antipolis, Parc Valrose, F-06108 Nice Cedex 2, France*

### ABSTRACT

The PICARD microsatellite mission will provide 3 to 4 years simultaneous measurements of the solar diameter, differential rotation and solar constant to investigate the nature of their relations and variabilities. The major instrument, SODISM, is a whole Sun imaging telescope of Ø110 mm which will deliver an absolute measure (better than 4 mas) of the solar diameter and solar shape. Now in Phase B, PICARD is expected to be launched by 2005. We recall the scientific goals linked to the diameter measurement with emphasis on the Helioseismology g-mode interest, present the instrument optical concept and present design, and give a brief overview of the program aspects.

### INTRODUCTION

SODISM/PICARD was first proposed in 1997 for the Space Station program before being accepted in 1998 as one of the two first CNES microsatellite missions. It covers two themes: solar influence on Earth climate and the internal structure of the Sun.

The solar energy is one of the major driving inputs for

terrestrial climate. Some evidences of correlations exist between surface temperature changes and solar activity. Global effects, such as diameter changes, large convective cells, the differential rotation of the Sun's interior and the solar dynamo at the base of the convective zone, can probably produce variations in the total irradiance, and therefore correlations. The use of these correlations is double: on one side prediction and on the other explanation of the past history of climate, like the Maunder minimum period.

To establish long-term links and trends between solar variability and climate changes, it is necessary to achieve not only high precision but also absolute measurements. This is what the diameter measurements of PICARD shall bring. Further, this high precision allows "instantaneous" monitoring of the diameter changes, i.e., with a proper orbit for the microsatellite, oscillations and, in particular, the gravity modes.

### SCIENTIFIC OBJECTIVES

#### Diameter and climate

From 1666 to 1719, Jean Picard and his student Philippe de la Hire measured the solar diameter, observed the sunspots and determined the Sun rotation velocity. Fortunately, these measurements covered the Maunder minimum and some time after. The data were re-examined by Ribes *et al.* (1987) who, after removing the seasonal variation of the solar diameter, obtained the annual means at 1 AU. These values, averaged for the Maunder minimum period, and after while the Sun recovered a significant activity, show a definitive difference of the order of 0.5 to 1 arcsec. It corresponds to a larger Sun diameter during the Maunder minimum. As expected, few sunspots were observed. Moreover, Picard's data also showed a slow down of the Sun rotation velocity at equator and significantly more sunspots in the south Sun hemisphere than in the north.

The solar constant measurements performed in space by the radiometers since 1978 were modeled using the sunspots number and faculae. This allowed to reconstruct the solar constant variation till 1610 (Lean, 1997). This showed that the solar constant experienced a significant decrease during the Maunder minimum. The temperature in the Northern Hemisphere has been also reconstructed for the same period. The cooling of this period is known as the Little Ice Age. The similarity of



*Fig. 1: Artist view of PICARD microsatellite, 60x60x80 cm<sup>3</sup> in size. Shown are the 3 instruments of the payload: SODISM, telescope and guiding, right, SOVAP, differential radiometer, center, and PREMOS (flux monitors) left, near the solar panels. In the back, one can see the electronics box supporting two S-band antennae and a solar pointer (acquisition maneuvers).*

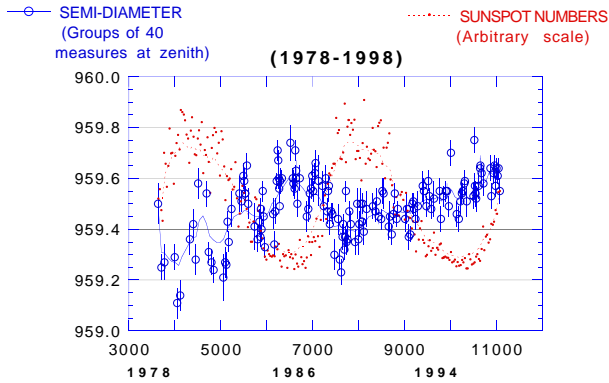


Fig. 2: Opposing phase observed between the sunspots number and the semi-diameter measured at CERGA's Astrolabe from 1978 to 1998 (by courtesy of F. Laclare).

the temperature and solar constant variations strongly suggests the Maunder minimum as the cause of the Little Ice Age. To assess this suggestion, climate models were run by Sadourny (1994) that showed the Maunder minimum as the possible cause of the Little Ice Age. Volcanic eruptions (major ones) also play a certain role, but their effects do not extent more than a few years.

As during the Maunder minimum, and suggested by Picard's data, the modern data of Sun diameter measurements and sunspots number, set together by Laclare *et al.* (1996), reveal a relation between the Sun radius and solar constant variations: it corresponds to an increase of the Sun radius for a decrease of the solar constant (cf. Fig. 2). Therefore, in order to establish experimentally without ambiguity the Sun constant and diameter relationship, we propose to operate from space by measuring simultaneously both quantities from the same platform and in non-magnetic lines or continua. The importance of the measurements for climatology is straightforward taking into account the Little Ice Age and the Maunder minimum events.

### What precision is required?

The total solar irradiance measure made by radiometers from space over the last 20 years, is excellent in relative terms ( $10^{-5}$ ) but poor in absolute. The amplitude of the variation over the cycle (0.1 %) is small and is about the same than the uncertainty on the absolute value from one instrument to the other. Prediction tendency of climate change from such data is not straightforward and adjustment of data sets of different origins an art (cf. Fröhlich and Lean, 1998). On the contrary, and if the relation irradiance-diameter is established by PICARD, the diameter measure which is precise, reproducible and absolute to 4 mas provides a proper — and quantified — sampling of the activity change over the cycle. Furthermore, the diameter measure will be done in the visible but also in the UV at 230 nm a wavelength band much more variable (6 to 8%) with the solar cycle and well known for its role in the chemistry of ozone, incidentally one of the possible links between solar activity and Earth climate.

### Diameter and oscillations

The other major objective of PICARD is to attempt the detection of the gravity modes (g modes) of the Sun. These modes are of prime importance to understand the structure and dynamics of the solar core which cannot be studied by using solar pressure modes (p modes) alone. So far the g modes have not been discovered by any set of instruments onboard the SOHO spacecraft (Appourchaux *et al.*, 2000). The 1- $\sigma$  upper limit to g-mode amplitude at around 200  $\mu$ Hz is typically 3.1 mm/s or 0.16 ppm (Appourchaux *et al.*, 2000). Given a velocity amplitude of 3.1 mm/s at 200  $\mu$ Hz, the displacement of the solar surface would be of about 5 m p-p which is equivalent to a variation of solar radius of about 6  $\mu$ arcsec. Although this level could be detected by PICARD, this is not the method used for detecting g modes. Nevertheless, it is worth noticing that MDI/SOHO was able — without an optimized telescope and imaging scheme as we have — to observe a 10  $\mu$ arcsec high frequency p-mode (5 min.) solar limb oscillation signal (Kuhn *et al.*, 1997).

With PICARD we want to detect intensity fluctuations at the solar limb that will perturb the equivalent solar radius signal. Appourchaux and Toutain (1998) reported to have detected p modes using the limb data of the LOI instrument. In some case the amplification with respect to full-disk integrated data is about 4, i.e. it means that a p-mode with an amplitude of 1 ppm in full disk is observed with an amplitude of 4 ppm at the limb (cf. Damé *et al.*, 1999). Analyses of Toutain *et al.* (1999) and Toner *et al.* (1999) confirmed such an amplification factor of 5. If we hope that the same amplification factor holds for the g modes, we may detect them faster with the limb data of PICARD than with the SOHO data. A pessimistic derivation gave 20 years for the detection of the first few g modes with SOHO (Fröhlich *et al.*, 1998). With PICARD we could seriously envisage detecting them in less than 2 years with the amplification factor above.

### THE SODISM TELESCOPE

SODISM is a simple telescope of useful diameter 110 mm. It forms a complete image of the Sun on a large, back thinned, CCD of 2K x 2K useful pixels. The pixel, 13.5  $\mu$ m, corresponds to 1.05 arcsec (at 1 AU) and the effective spatial resolution is also about an arcsec (at the limb). SODISM observes in 4 wavelengths bands the whole Sun (230 nm, 548 nm, 160 nm and Lyman alpha) and 2 calibration channels (cf. Table 1) accessible through the use of 2 cascading filterwheels, each with 5 positions.

### Operational modes

The main observing wavelength is 230 nm (8 nm bandwidth). It corresponds to a mostly flat UV continuum formed in the high photosphere. It is the best possible

choice of wavelength in the UV since it is sensitive to solar variations (about half of the MgII index variability for instance). It corresponds to the ozone bands where by chemical interaction in the stratosphere, the UV may affect the stratospheric dynamics and, consequently, the clouds coverage — which may be one of the paths of the Sun influence on the Earth's climate. In addition the limb darkening in this UV continuum is limited.

UV nominal mode	230 nm
Visible	548 nm
Active regions	160 nm
Prominences and ionosphere	Lyman alpha
CCD Flat Field	"Diffusion"
Scaling factor	"Star field"

Table 1: Observing and calibration modes of SODISM.

In addition, SODISM/PICARD observes 548 nm, which is near the center wavelength of the 100-nm bandpass used by DORAYSOL (Instrument for the solar diameter measurement with the Astrolabe used by Francis Laclare CERGA's group). The 160-nm and Lyman alpha filters are used for identification of active regions and prominences. This is essential to prevent activity manifestations to affect the "quiet" radius determination. This possibility to avoid, in the diameter computation, the pixels at the limb affected by faculae, active regions, prominences, sunspots or pores, is an essential feature of SODISM/PICARD since activity, therefore, does not add noise to the diameter measure.

The diffusion plates are simply used to monitor the CCD response and sensitivity (Flat Field). The CCD itself is a complete state-of-the-art system (EEV 4280 2K x 4K pixels back thinned and with frame transfer) hopefully developed in parallel of our program for the asteroseismology satellite program COROT.

Finally, specific to PICARD — and providing an absolute diameter reference better than 4 mas (milliarcsec)— is the "Star field" channel. It provides access to stellar fields in which stars' triplets (with a limit magnitude of 6 or so) of the HIPPARCOS reference catalog are imaged. It allows to scale our diameter measure and, if required, to identify and to follow any structural change in the focus or CCD dimensions which could affect the diameter measure.

### Optical concept and performance

SODISM has a sound optical concept allowing to achieve a near distortion free and dimensionally stable image of the solar limb. It has a symmetry of revolution (no complex optics — filters at normal incidence — nothing else than the two mirrors and a filter set in the optical path) and a single telescope-detector-guiding telescope support structure for common referencing and stability (cf. Fig. 3). The telescopes mirrors are made of SiC without coatings (reflectivity of 35–40 % in the UV and yet 20 % in the visible). The advantage is indeed

that the photometry will not change by aging and degradation of coatings since there are no coatings. Furthermore, the primary and secondary mirrors will help to remove 96% of the visible solar flux, preserving the filters from degradation and, due to the high conductivity of SiC, this flux will be evacuated to external radiators.

The instrument is 600 mm long. The primary-mirror diameter is 120 mm, 110 mm being used. The secondary-mirror diameter is 34 mm but only 24 mm are really used. For fine pointing needs, the primary mirror is mounted on a triad of piezoelectrics (at 120°). This allows to limit the blur during the nominal 1-second exposure to 0.1". Because of the diffraction and pixel size (13.5  $\mu$ m, 1.05") this prevents to affect the diameter measure (inflexion point measurement).

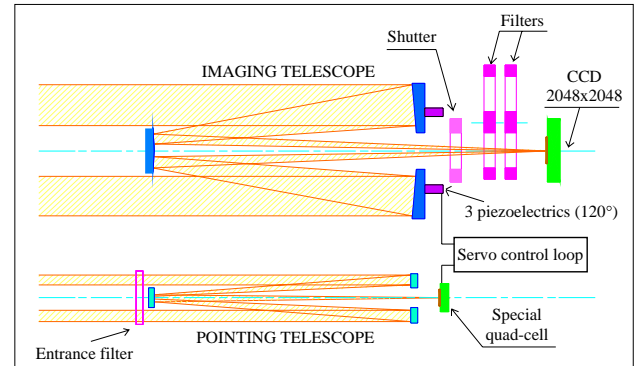


Fig. 3: Schematic of the optical setup of SODISM main imaging telescope and guiding telescope.

Note that although the SiC is very conductive, the flux concentration on the secondary mirror creates a gradient of temperature and thus a deformation of the mirror surface (small, a few nm) still sufficient to induce a residual systematic error of 12 mas between the "hot case" (the Sun) and the "cool case" (the stellar absolute calibration). This systematic error can be accounted in the data reduction process (others are, like the diffraction, 4 mas, the sampling, 7 mas, etc.) or compensated directly to an excellent precision by changing the temperature set point of the mirror from 20°C to 16°C. This 4°C difference (including a  $\pm 0.15^\circ$  tolerance on the settling point) would reduce the maximum error, in the whole field of view, to 0.4 mas.

Another important source of error is the CCD. Since the solar image (or stellar field) is formed on the CCD pixels, any change in the CCD dimensions will result in a change of the apparent solar diameter (or stellar distances). To minimize this error, the CCD (cooled at -40°C) is regulated to 0.2°C. Due to the silicon thermal expansion ( $\sim 2 \cdot 10^{-6}$  at -40°C), this may result in an error of 0.4 mas as well, more than half the error budget.

The mirrors and the CCD are indeed important sources of the error budget on the absolute diameter measure but not the only ones. The distance between mirrors and

with the focal plane is also very important to maintain the scaling factor. For these, a new and innovative approach using a carbon-carbon tube of high stability

and extremely low dilatation to link the optical elements and focal plane is used.

Error source	Nature of the error	Dilatation	Effect on radius
Structure	tube carbon-carbon: $2 \cdot 10^{-7}$ on 350 mm @ 0.5°C	$\pm 40$ nm	0.25 mas
	primary mirror to focal plane: C-C tube on 150 mm @ 0.5°C	$\pm 17$ nm	0.11 mas
	links (INVAR plates to tube, mirrors supports, piezos)	$\pm 20$ nm	0.12 mas
Optics	curvature of the primary mirror in SiC and thermal stability @ 0.2°C	12 nm	< 0.1 mas
	curvature of the secondary mirror in SiC and thermal stability @ 0.1°C	3 nm	< 0.4 mas
CCD	silicon thermal expansion $2 \cdot 10^{-6}$ on 12.5 mm @ 0.2°C	0.005 $\mu$ m	0.4 mas
Mean quadratic error budget ( $3\sigma$ )			0.65 mas

Table 2: Error budget of SODISM telescope on the solar radius measurement.

Measurements	Solar diameter, differential rotation and full Sun UV and visible imaging
Number of channels	6 (230, 548, 160 nm, Ly $\alpha$ , "Flat Field" & "Star Field")
Telescope focal length — solar image	2650 mm — Ø25 mm
Telescope optics	Primary Ø120 mm (used: 110 mm); Secondary Ø34 mm (used: 25 mm)
EEV-4280 back thinned CCD detector	2048x4096 13.5 $\mu$ m square pixels (frame transfer: 2048x2048 pixels used)
Guider acquisition range	1.2°
Guider nominal pointing range	$\pm 30''$
Guider servo bandwidths	0 to a few Hz (platform); a few Hz to 50 Hz (fine guiding on the primary)
Quad-cell image displacement sensitivity	Better than 0.01 arcsec
Piezo displacement range	$\pm 6$ $\mu$ m ( $\pm 1$ arcmin)
Pointing precision maximum residual jitter	0.1" (1 tenth of a pixel)
Absolute solar shape precision	Better than 4 mas (6 stars HIPPARCOS enhanced calibration in 2003)
Relative semi-diameter precision	Better than 1 mas

Table 3: Characteristics of SODISM.

### Resulting mechanical design

To provide a stable measurement of semi-diameters to a couple mas over the three to six years duration of the mission, SODISM/PICARD mechanical stability has to be excellent, intrinsically, and controlled. The design selected achieves mechanical and thermal stability because of the choice of a single monolithic structure — a tube of carbon-carbon — to link the SiC mirrors of the telescope and to the detector. The guiding telescope is in the same structure, its mirrors and the 4-quadrant detector being directly placed in the carbon-carbon tube. This new type of structure (developed for example by ALCATEL SPACE, cf. Bailly *et al.*, 1997) allows to reduce the thermal regulation to half a degree for a relative change of the diameter < 1 mas (1 thousand of a pixel). The isotropic property of carbon-carbon and a detailed knowledge of the experiment (calibration), will help to further gain, by modeling, a factor 100 to 1000 on the short term diameter variations (useful for the solar limb oscillations). This means that couples of  $\mu$ arcsec could be inferred, allowing a direct monitoring of limb oscillations.

Fig. 4 shows the structure design of the SODISM/PICARD telescope, with the carbon-carbon tube, the INVAR plates and SiC mirrors. Note also the small titanium feet which account for the dilatation of the

platform (instrumental plateau base plate in aluminum but with a carbon skin).

### PROGRAM AND MISSION ASPECTS

The PICARD's system uses most of the basic components of the CNES microsatellite product line, namely, the ground segment (MIGS) made of the "Centre de Contrôle Microsatellites" (CNES Toulouse), a band S station (and most probably a complementary station at high latitude) and the flight microsatellite segment. These components will be qualified by the first microsatellite mission of the product line, namely, the DEMETER mission. The PICARD system is operated mostly the same way as DEMETER and, in this way, confirms the generic character wanted and developed for the microsatellite product line.

#### Orbit

The PICARD's mission requires, ideally, an orbit with constant viewing of the Sun or, at minimum, with limited or short duration eclipses. The expected mission lifetime is 3 to 4 years with a possible extension to 6 years. Launch opportunities are essentially Sun Synchronous Orbits (SSO) with local time 6:00–18:00 (little or no eclipses). Several scenarios are still under

consideration for the PICARD flight which is not expected before 2005 (the launch date and expected life time are important since the diameter/constant relationship will definitively be better determined during the near linear part of the rising cycle than at minimum when the "constant" is mostly "constant"...). If 4 years can be envisaged based on the experience of the first microsatellites, and since our payload is not expected to degrade (telescope with SiC mirrors, etc.), a launch in 2005 is then possible.

Brief or non-eclipsing Sun-synchronous viewing orbits are essential in order to achieve both the thermal stability for the absolute long-term diameter measurement and the near continuous sampling for the long periods g-mode oscillations. At present launch is planned with a dedicated DNEPR Russian rocket on a 750 km SSO 6:00–18:00 orbit, which means short eclipses during 3 months or so over a year and limited to a few minutes up to 17 minutes at maximum.

### Pointing needs

The pointing needs on the PICARD microsatellite platform (for the scientific measure) is a pointing in the Z axis (telescope axis), towards the Sun, with a precision of  $\pm 0.01^\circ$ . This performance will be achieved by the attitude control system using a pointing-signal information provided by the payload (from the SODISM guiding telescope: pointing differences between the telescope and the Sun center direction). This, by itself, illustrates nicely the optimization capacity offered by the microsatellite system.

Pointing needs also imply a specific configuration of the stellar sensors (two heads) to preserve a permanent stellar pointing calibration along the orbit (stellar calibration need for the SODISM telescope-scaling factor).

### Platform characteristics

To the exception of the attitude control system, the microsatellite platform for PICARD is very similar of that of DEMETER. Globally, the adaptations are reasonable (in cost and complexity) and confirm the right choice of recurring technologies in the initial microsatellite product line.

Table 4 summarizes the essential characteristics of the present PICARD's microsatellite mostly derived from the microsatellite product line. To the exception of the power requirement, somewhat critical, PICARD's needs are well within the microsatellite possibilities.

### Payload characteristics

Table 5 summarizes the mass, power and nominal telemetry characteristics of the PICARD mission. Note that the PICARD Mission Center will normally be operated by the Royal Meteorology Institute of Belgium and that, most probably, antennae (S band) in Toulouse and Kiruna will be used for telemetry needs (about 1.5 Gbits per day). Depending on the data compression scheme selected, a higher telemetry rate (1.9 Gbits per day) could require a third antenna.

### ACKNOWLEDGEMENTS

We are thankful for their support to the mission to the CNES Microsatellite Division and Direction des Programmes and, in particular, to B. Tatry, C. Bouzat, J-Y. Prado, F. Dulac and N. Papineau, and would like to acknowledge the PICARD project and scientific teams (10 collaborators, 27 Co-Investigators) whom are doing a remarkable work towards a successful mission.

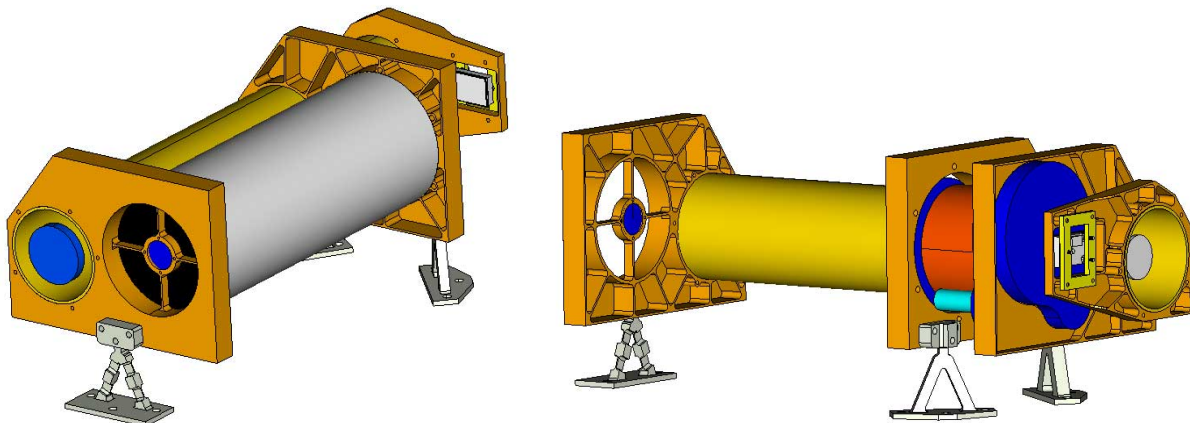


Fig. 4: Mechanical structure of the SODISM/PICARD telescope (350 mm between the primary and secondary mirror and 150 mm between the primary and the CCD surface). Note the 3 INVAR plates linked together by a 550-mm long carbon-carbon tube of Ø100 mm. The primary mirror is mounted on 3 piezoelectrics driven by a guiding telescope itself placed inside the C-C tube. The CCD (cooled to  $-40^\circ\text{C}$ ), is uncoupled of the INVAR plate by a Cordierite support.

Characteristics	PICARD Microsatellite
Size (cm <sup>3</sup> ) [L x W x H]	60 x 75 x 80
Mass (kg)	Platform (with lest): 68 kg — Payload: 42 kg max Total 110 kg (for 120 kg nominal: 10 kg margin)
Power (w)	Platform: 30 W (average on an orbit) — Payload: 42 W (average on an orbit) Total: 72 W
Pointing accuracy	3 axis stabilized, 0.1°
Pointing stability (platform)	0.01°
Pointing stability (SODISM)	0.1" (active pointing control on the primary mirror)
Mass Memory	1 Gbits
Telemetry flow	400 Kbits/s (1.5 Gbits/day)
TC (commands)	10 Kbits (immediate or delayed)
Orbit restitution	1 km
Onboard datation	< 0.5 s (TU difference)

Table 4: Performances of PICARD microsatellite.

Characteristics	PICARD Payload	SODISM	SOVAP	PREMOS	Electronics boxes (2)
Mass (kg)	41.8	17.9	5.8	4.1	10 & 4
Size (cm <sup>3</sup> )	60x60x30 18x19x19*	60x27x28	35x15x15	30x9x20	<16x26x26 <18x19x19*
Power (W)	32.9	18.4	10.1	4.4	NA
Thermal Control (W)	9.0	9.0	—	—	NA
Average Telemetry (Mbits/day)	1510	1500	5	5	NA

\* This electronic box is placed under the microsatellite platform

Table 5: Characteristics of PICARD model payload

## REFERENCES

- Appourchaux, T. *et al.*, Observational Upper Limits to Low-Degree Solar g-Modes, *Ap. J.* 538(1), 401-414 (2000).
- Appourchaux, T. and Toutain, T., in *Sounding Solar and Stellar Interiors*, IAU Symposium 181 (Poster Volume), Eds. J. Provost and F.X. Schmider, 5 (1998).
- Bailly, B. *et al.*, High Stability Carbon/Carbon Telescope Structure, *Proc. ICSO'97, CNES International Conference on Space Optics*, Ed. G. Otrio, S4, 1–11 (1997).
- Damé, L. *et al.*, PICARD: Simultaneous Measurements of the Solar Diameter, Differential Rotation, Solar Constant and their Variations, in *Symposium on Helioseismology and Solar Variability*, *Adv. in Space Research* 24(2), 205–214 (1999).
- Fröhlich, C. and Lean, J., The Sun's total irradiance: Cycles, trends, and related climate change uncertainties since 1976, *Geophysical Research Letters* 25(23), 4377 (1998).
- Fröhlich, C. and the Phoebus Group, in *Structure and Dynamics of the Sun and Solar-like Stars*, *Proceedings of the SOHO 6 / GONG 98 workshop*, Boston, USA, ESA SP-418, 67 (1998).
- Kuhn, J.R. *et al.*, Precision Solar Astrometry from SOHO/MDI, in *Sounding Solar and Stellar Interiors*, IAU Symposium 181, Eds. J. Provost and F.X. Schmider, 103–110 (1997).
- Laclare, F., Delmas, C., Coin, J.P. and Irbah, A., Measurements and Variations of the Solar Diameter, *Solar Physics* 166, 211–229 (1996).
- Lean, J., The Sun's Variable Radiation and its Relevance for Earth, *Annu. Rev. Astron. Astrophys.* 35, 33–67 (1997).
- Ribes, E., Ribes, J.C. and Bartholot, R., Evidence for a Larger Sun with a Slower Rotation during the Seventeenth Century, *Nature* 326, 52–55 (1987).
- Sadourny, R., Sensitivity of Climate to Long-term Variations of the Solar Output, in *The solar engine and its influence on terrestrial atmosphere and climate*, Ed. E. Nesme-Ribes, NATO ASI Series I, vol. 25, 479–491, Springer Verlag (1994).
- Toner, C.G., Jefferies, S.M. and Toutain, T., Increasing the Visibility of Solar Oscillations, *Ap. J.* 518(2), L127-L130 (1999).
- Toutain, T., Berthomieu, G. and Provost, J., Light perturbation from stellar nonradial oscillations: an application to solar oscillations, *A. & A.* 344, 188-198 (1999).